

UC Davis

Research Reports

Title

Improvement of Thermal Stability of Li-Ion Batteries by Polymer Coating of LiMn₂O₄

Permalink

<https://escholarship.org/uc/item/9gp9x6x4>

Authors

Stroeve, Pieter
Vidu, Ruxandra

Publication Date

2004-05-01

Peer reviewed

**IMPROVEMENT OF THERMAL STABILITY OF LI-ION
BATTERIES BY PLOYMER COATING OF LiMn_2O_4**

UCD-ITS-RR-04-11

May 2004

by

Pieter Stroeve
Department of Chemical Engineering and Materials Science
and
Institute of Transportation Studies
University of California, Davis 95616, USA
Ph (530) 752-8778
Fax (530) 752-6572
pstroeve@ucdavis.edu

and

Ruxandra Vidu

Institute of Transportation Studies
One Shields Avenue
University of California
Davis, California 95616
Tel: 530-752-0247 Fax: 530-752-6572
<http://www.its.ucdavis.edu/>
email: itspublications@ucdavis.edu

**Improvement of Thermal Stability of Li-ion Batteries
by Polymer Coating of LiMn_2O_4**

Ruxandra Vidu and Pieter Stroeve*

*Department of Chemical Engineering and Materials Science,
University of California, Davis,
Davis, CA 95616, USA,*

*Author to whom correspondence should be addressed

E-mail: pstroeve@ucdavis.edu

Fax: +1-530-752-8778

Phone: +1-530-752-8778

Abstract

A new approach has been used to minimize surface degradation of the LiMn_2O_4 cathode in lithium ion batteries by using surface modification. LiMn_2O_4 particles used as active material in cathode fabrication were modified by surface adsorption of poly(diallyldimethylammonium chloride) (PDDA). Adsorption and electrochemical performance of the modified cathode material were characterized and compared with that of the untreated LiMn_2O_4 -based cathode. Transmission Electron Microscopy (TEM), Scanning Electron Microscopy (SEM) and Energy Dispersive X-ray analysis (EDAX) analyses confirmed the formation of a thin polymer film on the surface of LiMn_2O_4 particles. The modified LiMn_2O_4 -based cathode showed improved stability during charge/discharge cycling in organic electrolyte at room temperature. Further, the measured capacity fading *after storage* at elevated temperature decreased. Capacity fading measured on cathodes made of PDDA-coated LiMn_2O_4 powder was smallest for cathodes obtained from powder coated in solutions containing between 30 and 50 mM PDDA. *In situ* AFM observation of the cathodes at room temperature showed minor changes in surface topography during a potential cycle. Our hypothesis is that the adsorbed polymer layer blocks surface reactions that cause degradation. The present method for surface modified LiMn_2O_4 (SM-LMO) particles extends the lifetime of the lithium-ion battery by arresting the Mn^+ dissolution, thereby increasing the battery stability.

Key Words: Lithium Battery, Cathode, LiMn_2O_4 , Polymer Film, Electrochemical Atomic Force Microscopy.

INTRODUCTION

Spinel LiMn_2O_4 is considered to be the most promising alternative cathode material for the new generation of lithium ion batteries in terms of its low cost, low-toxicity and easy manufacture. Recent developments in LiMn_2O_4 based cathodes for lithium ion batteries fall in two major categories: preparation of thin films (by sputtering, electron beam evaporation, pulse-laser deposition, chemical vapor deposition, sol-gel etc) and substitution of a small fraction of manganese ions with other metal cations (e.g. Cr, Al, Co etc). More recently, surface modifications to enhance cell-surface interactions are under study due to the major role played by the interface in battery processes [1-8].

Studies conducted to clarify the mechanism of lithium battery deterioration [9-23] have verified several theories on capacity fading mechanisms. Processes involved in capacity fading occur through a combination of various processes at elevated temperatures, which include: electrolyte decomposition, dissolution of LiMn_2O_4 , irreversible phase and structure transition (i.e. Jahn-Teller distortion at the discharged state, transformation of an unstable two-phase structure in the high voltage region to a more stable single-phase structure through loss of MnO), and material loss of the loaded spinel and polarization loss due to cell resistance increase (i.e. high contact resistance at the spinel/carbon interface caused by Mn dissolution).

Surface modification techniques demonstrated beneficial effects on the electrochemical stability of LiCoO_2 and LiMn_2O_4 active material (either in a film or powder form). Studies on LiCoO_2 coated with different metal oxides Al_2O_3 [1, 3, 5, 7], MgO [5, 24], SnO_2 [5] and LiMn_2O_4 [25] have proven increased electrochemical performances.

In the case of sol-gel coating of LiCoO_2 with Al_2O_3 [1], the original specific capacity of 174 mAh/g (vs. lithium metal) of the cathode is preserved and an excellent capacity retention (97 % of its initial capacity) between 4.4 and 2.15 V after 50 cycles has been obtained. Similar results have been obtained by other coating methods [5] when the Al_2O_3 coating layer was amorphous. Studies performed on LiCoO_2 films [3] have shown enhanced electrochemical properties in the Al_2O_3 -coated LiCoO_2 films than the bare ones. The improved cycling behavior of the coated films is caused by the suppression of cobalt dissolution from the LiCoO_2 thin films, with the formation of a thin-film solid solution layer ($\text{LiCo}_{1-x}\text{Al}_x\text{O}_2$) [3] between the LiCoO_2 cathode and liquid electrolyte. Although similar results were observed in LiCoO_2 powders and films, i.e. enhanced cycle performance after coating with a thin-film aluminum-oxide coating, the Al_2O_3 -coated or uncoated LiCoO_2 thin films shows negligible *c* axis expansion in comparison with the LiCoO_2 powder.

The electrochemical performances of oxide-coated LiCoO_2 depend on the metal oxides [5]. MgO -coated LiCoO_2 cathode shows very good electrochemical stability up to a charge cutoff voltage of 4.7 V [24] while Al_2O_3 -coated LiCoO_2 is electrochemically stable up to 4.5 V, without decreasing its available specific capacity. However, SnO_2 -modified LiCoO_2 is stable only at low- charge cutoff voltages. Surface modification does not influence the phase transitions below 4.5 V but the phase transition at about 4.58 V is drastically suppressed. High specific capacity and cyclic stability obtained for oxide-modified cathodes are attributed to the dual role of the coating: 1) to protect the active material from direct contact with the acidic electrolyte and dissolution of Co^{4+} ions, and 2) to suppress the phase transition by supplying Mn^{2+} from MnO coating into the active material at low potentials that prevents vacancy ordering at high charge potentials.

Surface treatments of LiMn_2O_4 powder include coatings with inorganic lithium boron oxide glass (LBO) [26] and LiCoO_2 [25, 27] prepared by a sol-gel process. Based on the fact that Mn dissolution takes place at the interface of electrolyte and LiMn_2O_4 , the role of the coating is to protect the electrolyte from the catalytic effect of LiMn_2O_4 and to protect the LiMn_2O_4 particles from corrosion by HF.

It is clear that coating LiCoO_2 and LiMn_2O_4 active material with inorganic oxides can modify the properties of the surface exposed to the electrolyte solution and change the electrochemical properties of the cathode. Oxide-based coatings have shown that the modification of the cathode materials is an effective approach to stabilize the structure of the materials and improve the electrochemical performance. However, the available capacity of the coated material is lower than the active material due to the employment or formation of electrochemically inactive compounds in the coating layer as well as the low charge cutoff voltage of the half-cell.

Therefore, there is a challenge in the lithium-ion battery field to identifying the surface reactions and to find strategies to suppress capacity fading at high temperatures. In our previous work [15, 28], we used various surface sensitive techniques to study the complex reaction/dissolution process that assists the Li intercalation/deintercalation process during potentiostatic charging and discharging conditions. In this work, we report a novel organic coating method to enhance the performance of LiMn_2O_4 based batteries by surface modification on a molecular scale. Significant improvement in electrochemical properties of LiMn_2O_4 -based cathodes is obtained by applying a direct coating of PDDA on LiMn_2O_4 particles. Besides surface characterization tools such as SEM, EDAX and TEM, and traditional electrochemical characterization techniques employed in battery characterization, we used *in situ* electrochemical AFM under potential and temperature

control. This technique was initiated in our group [28] and proved to offer direct monitoring of the cathode surface under potential and temperature control. The development of a high-resolution *in situ* EC-AFM method for battery studies at elevated temperature provides a nanoscale understanding of the local redox reactions at cathode/electrolyte interface and enable us to speed up the process, to do predictive degradation studies and predict battery properties.

EXPERIMENTAL SECTION

Materials. Cathode wafers were prepared from LiMn_2O_4 (synthesized by Mitsubishi Chemical Corp.), acetylene black (Denki Kagaku Kogyo Co. Ltd.), and Teflon (Mitsui Dupont Fluoro Chemical Co. Ltd.). The polymers poly(diallyldimethylammonium chloride) (PDDA) was purchased from Polysciences, Inc. (Warrington, PA). The buffer solution used throughout the experiments was Tris 8.5 (5 mM Tris buffer, pH 8.5, purged with N_2). All chemicals were used as received without further purification. De-ionized water (resistivity $> 17.5 \text{ M}\Omega\text{-cm}$) was obtained from a Nanopure Reverse Osmosis Purification System from Barnstead (Dubuque, IA).

Coating Procedure A known amount of LiMn_2O_4 powder was first weighted and then 50 mM Tris 8.5 solution was poured over the powder. It was sonicated for 2 h in order to disintegrate the agglomerated powder and increase the surface area available for polymer adsorption. Then, a fixed volume of PDDA solution (10, 20, 30, 50, and 100 mM PDDA in Tris 8.5) was added and slowly mixed using a stir bar for another 2 h. The powder was separated with a centrifuge and dried for 2 h at 120°C . The powder was used to make the cathode wafers.

Sample Preparation Cathode wafers were routinely prepared by mixing 75 wt.% of PDDA-coated LiMn_2O_4 , 20 wt.% of acetylene black, and 5 wt.% of Teflon, and were kneaded to a flat sheet with a mortar and a pestle. A cathode wafer was punched out from the sheet into a disk 8 mm in diameter, weighted and pressed on an aluminum metal mesh,

which was used as the working electrode in the electrochemical measurements. Then, the wafer was dried at 120°C in a vacuum oven for 2 hours to remove excess water and water vapor, which could react with the electrolyte.

Sample Characterization

The PDDA amount adsorbed on LiMn_2O_4 powder from PDDA solutions with various concentrations was obtained using a UV-Vis spectrophotometer (Varian Analytical Instruments, CA). The difference in the PDDA concentrations in solution before and after equilibration of the powder was measured with UV-Vis. The PDDA amount adsorbed on LiMn_2O_4 powder were converted into the amount of polymer adsorbed per gram of LiMn_2O_4 powder.

For electrochemical studies, a beaker-type, three-electrode cell was used inside an Argon atmosphere glove box. The working electrode was placed in the cell with two pieces of pure Li metal (Alfa Aesar), which were used as the counter and the reference electrodes. The electrolyte used for electrochemical measurements contained 1 mol of LiPF_6 in a mixed solvent of ethylene carbonate (EC) and diethyl carbonate (DEC). The proportions for EC:DEC were 3:7 by volume (Mitsubishi Chemical Corp.).

Charge/discharge properties of the electrochemical cell were measured with a Model HJ-201B charge/discharge unit (Hokuto Denko Corp.) in the voltage range of 3.2 V and 4.3 V. Cyclic voltammetry was carried out with a Model AFCEBP1 bipotentiostat (Pine Company) between 3.2 V and 4.4 V at the sweep rate of 10 mV/min. After charging, the cathode and a Li metal separated by a polyethylene sheet were placed in a Teflon bottle and immersed in fresh electrolyte, and stored in an oven at 70°C for one week. The cathode

was then extensively rinsed with pure DMC. *Before* and *after storage*, the electrochemical properties of the cell were determined. *After storage*, new Li metal was used to assemble the battery. All sample preparations and measurements were conducted at room temperature (25 °C).

Energy Dispersive X-ray analysis (EDAX) was carried out on an Oxford Link 1000 Scanning Electron Microscope (SEM) with an Isis EDS detector with a beryllium window and 139 eV resolution. All data were taken under the same conditions to avoid any scaling issues.

Transmission Electron Microscopy (TEM) was performed on a Topcon 002B, 200KV. Transmission Electron Microscopy was used to study the PDDA coating on nanoparticles. The method used for dispersing the powder for TEM observation consisted of grinding the powder in methanol solution and then transferred on a carbon coated copper TEM grid.

The surface of the cathode was observed by atomic force microscopy (AFM, Nano Scope IIIA, Digital Instruments) using various imaging modes in air and in electrolyte. Commercially available triangular gold-coated cantilevers with pyramidal tips of 0.05 N/m force constant were used for AFM imaging in contact mode. To correct for tilt and bow, images were typically processed using the imaging software of the instrument.

The electrochemical cell used in EC-AFM is similar to the cell used for other electrochemical measurements, e.g. it consists of cathode material as the working electrode and two lithium sheets as counter and reference electrodes [28]. Active electrochemical control and simultaneous observations of the surface reactions were carried out in the AFM set-up. The applied potential/current is monitored through a bipotentiostat and a thermostat controls the temperature of the sample that was heated up by a small device, which has

been specially designed to fit the AFM scanner head. The sample was attached to the holder using double-sided conductive tape. The electrochemical cell consists of glass and was placed over the sample. An O-ring sealed the electrolyte. The assembly of the cell was done inside the argon atmosphere glove box at room temperature. All measurements were conducted at room and elevated temperature. Galvanostatic discharge and charge curves as well as cyclic voltammetry have been measured prior to *in situ* EC-AFM.

In a typical EC-AFM experimental run the surface was first observed at a constant open-circuit voltage (OCV). Then, the surface was monitored under potential control at different potentials within the range from 3.2 to 4.5 V vs. Li/Li⁺ in LiPF₆ electrolyte in order to image the changes in surface structure and topography of the cathode during charging and discharging process. The surface scans were performed at several resolutions in order to analyze both global and local information.

RESULTS AND DISCUSSION

Adsorption

UV-vis spectroscopy analysis was performed in order to measure the equilibrium adsorption of PDDA on LiMn_2O_4 powder. Table 1 presents the PDDA amount adsorbed on LiMn_2O_4 powder. The initial PDDA concentration (c_i) and the final PDDA concentration (c_f) are shown in Table 1. The amount of PDDA adsorbed on LiMn_2O_4 powder varies with the equilibrated PDDA concentration in solution with a parabolic behavior up to about 10.8 mM in c_f . The amount of PDDA adsorbed on the powder decreases slightly for a PDDA concentration of $c_f = 34$ mM and then continues to decrease at $c_f = 97$ mM. Thus the adsorption data show non-Langmuirian behavior, which is a phenomena often observed for polymer adsorption [29]. For convenience, in the next sections, we refer to the concentrations of PDDA in terms of the initial treatment concentration c_i reported in Table 1.

Electrochemical measurements

The electrochemical tests have been performed on cathode samples obtained by adsorbing a thin, molecular film of PDDA on the LiMn_2O_4 powder. Charge/discharge properties of the electrochemical cell were measured *before* and *after storage*. The electrochemical properties of the cathode were first determined *before storage*. These results were reproducibly obtained in a subsequent set of *before* and *after storage* experiments. The *after storage* measurements refers to data collected on samples after storage in a charged state at 70 °C for one week.

For comparison, cyclic voltammetry and charge/discharge curves of standard (uncoated) LiMn_2O_4 based cathodes are presented in Fig. 1. Figure 1 a shows that there is no difference in capacity measurements between non-modified and PDDA-modified cathodes *before storage*. Charge/discharge curves and the variation of the measured capacity with the number of cycles for the cathodes obtained from surface modified lithium manganese oxide (SM-LMO) powder in 50 mM PDDA solution is shown in Figure 2. For larger PDDA concentrations, e.g. 200 mM PDDA, the capacity is lower than the standard LiMn_2O_4 based cathode and the interfacial resistance is high. Further, we explored the cathodes made of LiMn_2O_4 powder coated with PDDA in solutions of concentration ranging from 10 to 100 mM PDDA solutions. Capacity measurements were performed for samples obtained in PDDA solutions of various PDDA concentrations (10, 20, 30, 50 and 100 mM solutions). The capacity of the new cathodes is generally good, within the range of standard LiMn_2O_4 -based cathodes. The stability of capacity after 5-10 cycles was also good, with a capacity lost of 9.3 ± 5.3 % (Fig. 3).

The electrochemical tests *before* and *after storage* is presented in Fig. 4. Generally, the charge/discharge curves of the standard LiMn_2O_4 -based cathode after storage show 18-20 % loss of the initial capacity. After one week of storage, the discharge capacity measured at the same current density decreased. In addition to the capacity fading, hysteresis between charge and discharge curves became larger after storage. Since the hysteresis corresponds to the resistance of the cell, it is clear that after storage the resistance of the spinel cathode increased. Coating the LiMn_2O_4 powder with PDDA resulted in an improved stability of the cathode during charge/discharge cycling in organic electrolyte at room temperature (Fig. 4). Also, Figure 4 shows that there is no difference in capacity measurements between non-modified and PDDA-modified cathodes *before storage*, just as

was seen in Fig. 1c. After storage, the capacity fading was significantly reduced and the capacity lost after storage was only 6 % for cathodes made of PDDA-coated LiMn_2O_4 powder. In this case, the capacity fading is minimum for cathodes obtained from powder coated in solution containing 30 and 50 mM PDDA. Although the hysteresis between charge and discharge curves became larger after storage, the magnitude of the displacement is lower than that measured on standard cathode wafer. Moreover, the capacity curve obtained after storage for cathodes made of powder coated in a solution containing 30 mM PDDA retained the same aspect before storage, which is a significant improvement relative to the standard LiMn_2O_4 cathodes. Thus we see from Figs 1-4 that coating the LMO particles with polymer retains the room temperature performance of the LiMn_2O_4 based cathodes, while the same cathodes show improved thermal stability *after storage* at elevated temperatures.

Transmission Electron Microscopy

Transmission electron microscopy was used to characterize the polymer coating on the LiMn_2O_4 particles. A typical electron diffraction micrograph is shown in Fig. 5. The TEM observation revealed the presence of polymer. However, it is not clear how uniform the polymer coating is. The TEM image shows that the PDDA film embedded the crystalline LiMn_2O_4 particles, i.e. the PDDA is not simply mixed with LMO particles but coated on the LMO powder. Additional investigations using the Scanning Electron Microscopy (SEM) were carried out in order to characterize the polymer coating.

Electrochemical Atomic Force Microscopy

Although the spinel LiMn_2O_4 oxide for rechargeable Li ion batteries has been intensively studied by electrochemical methods, there is no systematic and comprehensive study by AFM or EC-AFM of the cathode surface in organic electrolytes. In this work, the surfaces of the cathode were observed by atomic force microscopy (AFM, Nano Scope IIIA, Digital Instruments) in wet and dried state. We investigated the effect of surface reaction at the cathode/electrolyte interface on the mechanism of capacity fading at elevated temperatures by *in situ* Electrochemical Atomic Force Microscopy (EC-AFM). First, the cathode surface was imaged in dried state. Figure 6 shows the AFM in air in contact mode of the cathode surface in air. Samples were obtained from PDDA coated LMO powder in solution containing 30 mM (Fig. 6, top) and 100 mM PDDA (Fig. 6, bottom). The cathode surface appears smooth and homogeneous, typical to a well-mixed composite material. However, for high PDDA concentration, i.e. 100 mM PDDA, several “lake-like” spots were observed (Fig. 6, bottom, scan size 7.08 x 7.08 μm). These spots are most likely areas containing excess PDDA polymer. The AFM results show that when a concentrated PDDA solution is used for coating, the non-homogeneity of the PDDA coating. The non-homogeneity may be associated with the particle size distribution.

In the presence of the electrolyte, the binder and active material areas were identified by comparing the particular topography of each phase present in the surface with that observed in air. We studied the local redox reaction by *in situ* EC-AFM imaging of the cathode surface in organic electrolyte under potential control at room temperature and elevated temperature. We investigated the effect of surface reaction at the cathode/electrolyte interface during charging/discharging cycles. Figure 7 shows the *in situ* EC-AFM of SM-LMO based cathode (30 mM PDDA solution) in 1 M LiPF_6 + EC/DEC

electrolyte during charging from $E = 3.5$ V to $E = 4.5$ V, holding at 4.5 V for 1/2 h and discharging back to $E = 3.5$ V, at room temperature. A sketch of the potential variation was inserted to help understanding the EC-AFM image acquisition. In this case, no significant changes in surface topography were detected.

Figure 8 shows the *in situ* EC-AFM of SM-LMO based cathode (30 mM PDDA solution) in 1M LiPF₆ + EC/DEC electrolyte during charging from $E = 3.5$ V to $E = 4.5$ V, holding at 4.5 V for 1/2 h and discharging back to $E = 3.5$ V, at elevated temperature (55 °C). The stability of the surface topography is noteworthy, which supports the improved electrochemical behavior observed after storage (Fig. 4). Figure 9 shows the *in situ* EC-AFM of SM-LMO based cathode (100 mM PDDA solution) in 1M LiPF₆ + EC/DEC electrolyte during charging from $E = 3.5$ V to $E = 4.5$ V, holding at 4.5 V for 1/2 h and discharging back to $E = 3.5$ V, at room temperature. Slightly unstable, the cathode surface shows an increase in surface roughness during charging and a smoothing trend during discharging. This result is consistent with the delithiation-lithiation reaction that relates to the charging/discharging process but the changes in surface topography are significant at this observation scale. Figure 10 shows the *in situ* EC-AFM of SM-LMO based cathode (100 mM PDDA solution) in 1M LiPF₆ + EC/DEC electrolyte during charging from $E = 3.5$ V to $E = 4.5$ V, holding at 4.5 V for 1/2 h and discharging back to $E = 3.5$ V, at elevated temperature (55 °C). Significant and irreversible changes take place during charging, which clearly account for the decrease of the measured capacity after storage.

Scanning Electron Microscopy (SEM) and Energy Dispersive X-ray Analysis (EDAX)

High resolution SEM combined with EDAX offer detailed information on both morphological and compositional aspects of the coated particles. For comparison, Fig. 11

presents the standard LiMn_2O_4 powder, before coating. Figures 12 presents the EDAX data along with the SEM images of PDDA coated powder samples. The Mn and O peaks are clearly visible. Additionally, we mapped the particles for elements such as C, which is contained in PDDA but not in the nano particles. The carbon distribution is very weak but in agreement with the low amount of PDDA present on the nano particles. It appears from Fig. 13 that there are only slight differences between the amounts of C present on LMO particles treated at different concentrations. Simulation runs for a monolayer of PDDA film on a LiMn_2O_4 particle of 300 nm in diameter show C, Mn and O spectra similar to that presented in Fig. 13.

The significant improvement of thermal stability of Li-ion batteries by polymer coating of LiMn_2O_4 is probably due to the “membrane” like behavior of the polymer. The coating should protect the LiMn_2O_4 particle surface from direct contact with the electrolyte and possibly blocks or reduces surface reactions that are in part responsible for the capacity fading in Li-ion batteries [15]. Our previous results suggest a surface degradation mechanism in uncoated cathodes wherein the LiPF_6 salt dissociates reversibly to LiF and PF_5 . The PF_5 , in turn, reacts with the manganese oxide on the LiMn_2O_4 surface to form manganese difluoride on the surface and soluble products in the electrolyte. The soluble products in the electrolyte are probably POF_3 and PO_2F_2 [15]. We propose here that the PDDA polymer coating may inhibit the surface degradation by blocking access to the surface and therefore lead to improved thermal stability of the Li-ion battery.

CONCLUSIONS

Coating with a thin layer of PDDA modified LiMn_2O_4 particles used as active material in cathode fabrication. Coating properties and electrochemical performance of the modified cathode material were characterized and compared with that of the standard (uncoated) LiMn_2O_4 -based cathode. SEM and EDAX analyses confirmed the formation of a thin polymer film on the surface of LiMn_2O_4 particles. The PDDA modified LiMn_2O_4 – based cathode showed improved stability during charge/discharge cycling in organic electrolyte at room temperature. The measured capacity fading after storage also decreased. Capacity fading measured on cathodes made of PDDA-coated LiMn_2O_4 powder was smallest for cathodes obtained from powder coated in solutions containing 30 and 50 mM PDDA.

EC-AFM studies on Li-ion battery electrodes offered complementary information needed to understand the surface processes on the cathode. The *in situ* AFM observation of the surface modified cathodes at room temperature shows minor changes in surface topography that follow the potential cycle if the coating is done with 30 or 50 mM PDDA solutions. During a charging/discharging cycle, surface changes observed by EC-AFM on modified cathode were significantly smaller than on the standard cathode. Our hypothesis is that the PDDA layer blocks surface reactions that cause degradation.

Acknowledgments

This research was supported by EISG No. 52507A/01-21

Table 1. The amount of PDDA adsorbed on LiMn_2O_4 powder at equilibrium (c_i is the starting (initial) concentration of PDDA and c_f is the equilibrium (final) concentration).

<u>c_i (mM)</u>	<u>c_f (mM)</u>	<u>PDDA adsorbed on powder (mol/g)</u>
10	0.46	5.53 E-7
20	4.14	9.17 E-7
30	10.82	1.09 E-6
50	34.58	8.01 E-7
100	97.56	6.30 E-7

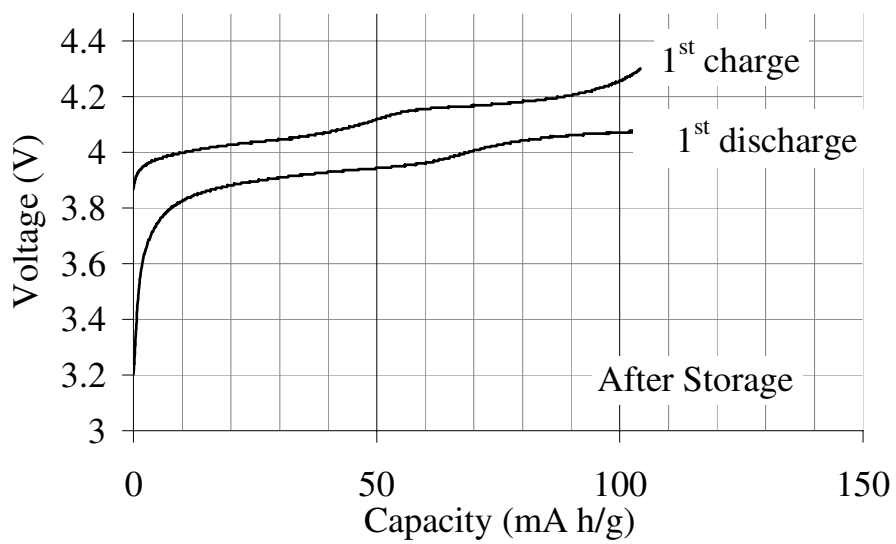
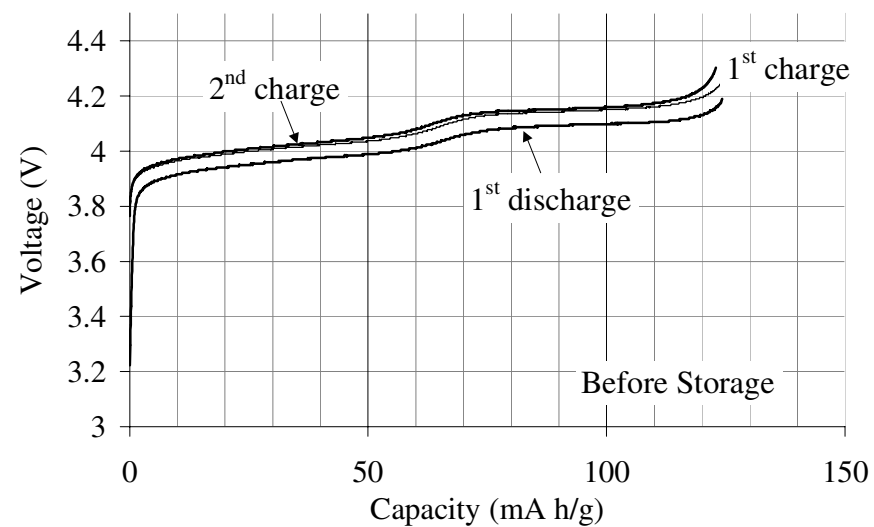


Figure 1. Charge/discharge curves and of LMO-based cathode in 1 mol of $\text{LiPF}_6 + \text{EC/DEC}$.

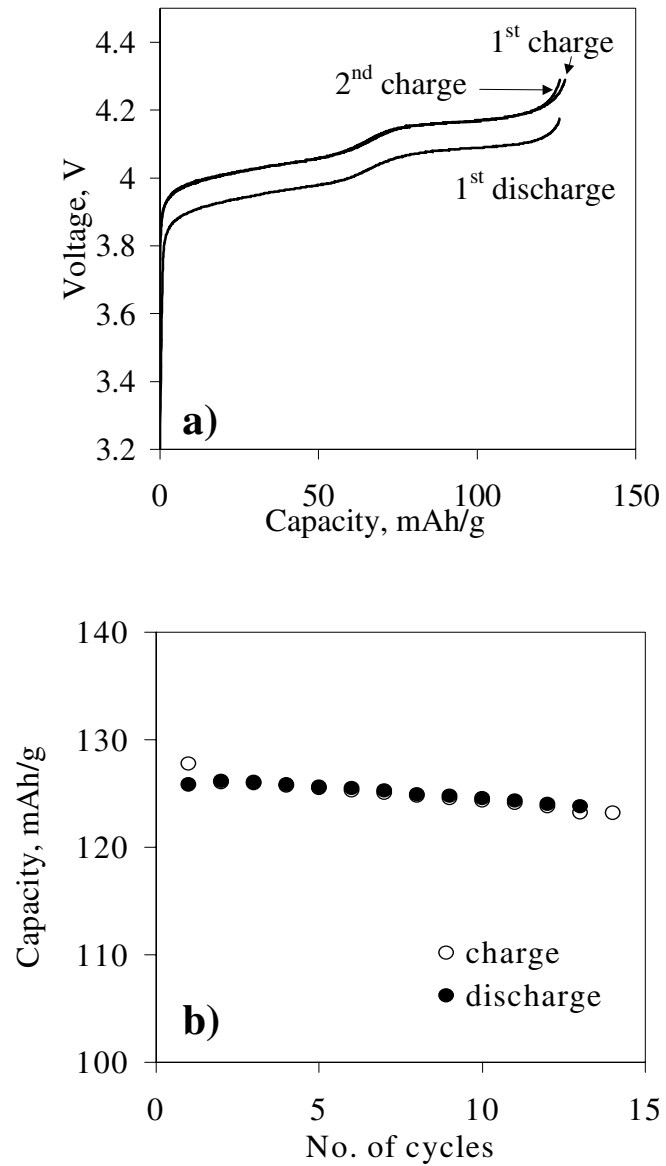


Figure 2. Charge/discharge curves (a) and the variation of the measured capacity with the number of cycles (b) for the cathode obtained from PDDA coated powder in 50 mM PDDA solution.

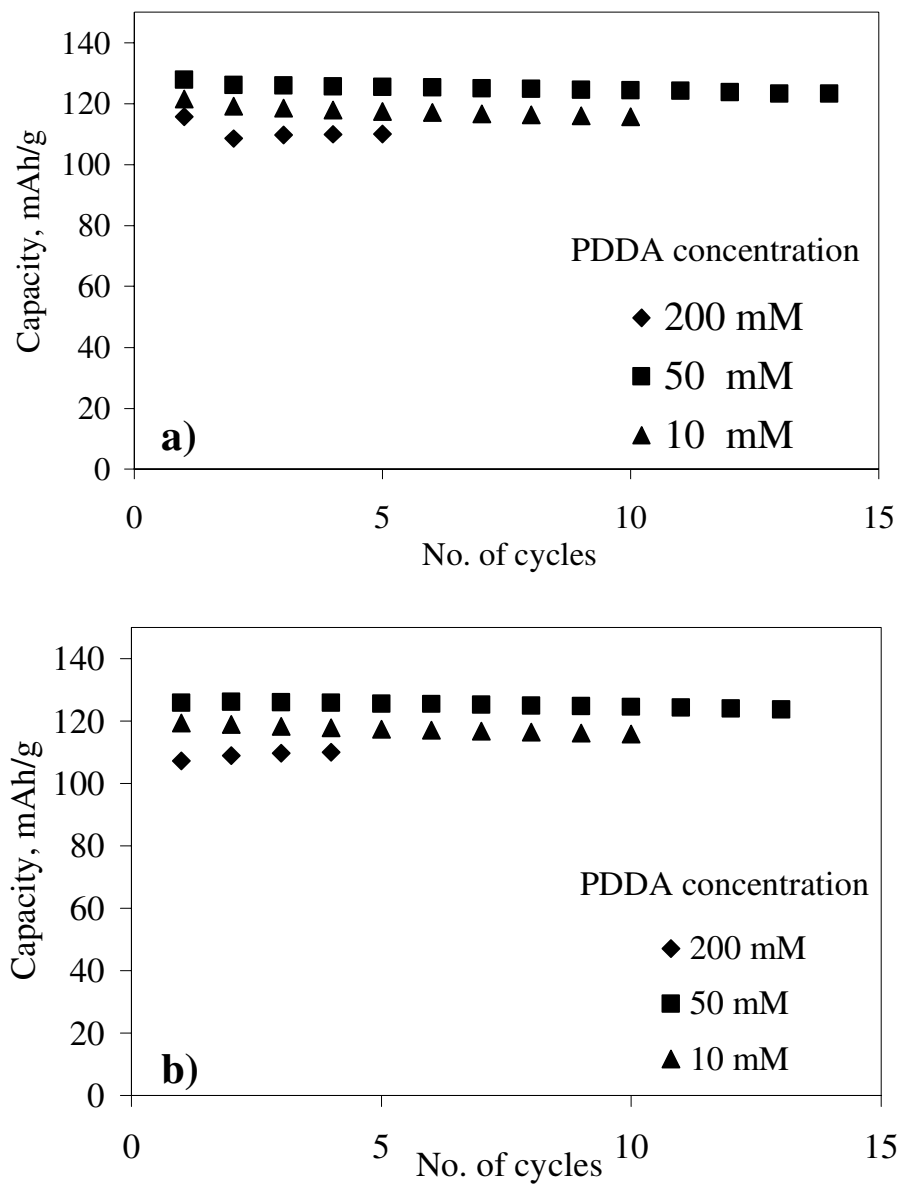


Figure 3. Variation of the measured capacity during charging (a) and discharging (b) with the number of cycles for the cathodes obtained from the PDDA coated powder.

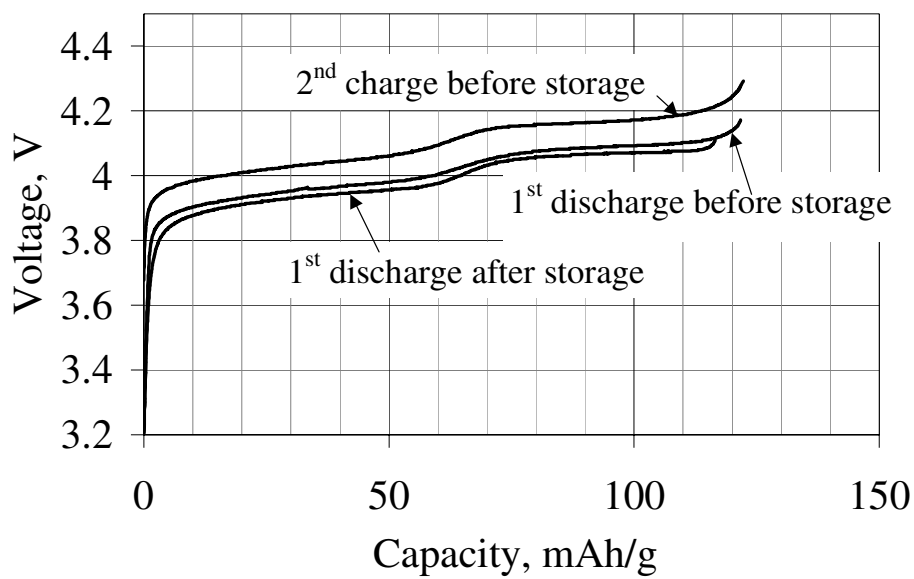


Figure 4. Charge/discharge curves of SM-LMO (30 mM PDDA) -based cathode before (a) and after (b) storage.

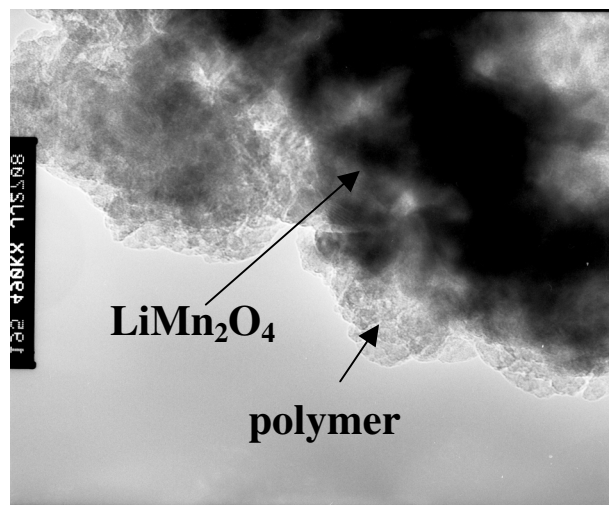


Figure 5. TEM image (x49K) of typical SM-LMO powder indicating crystalline LiMn_2O_4 region and polymeric film.

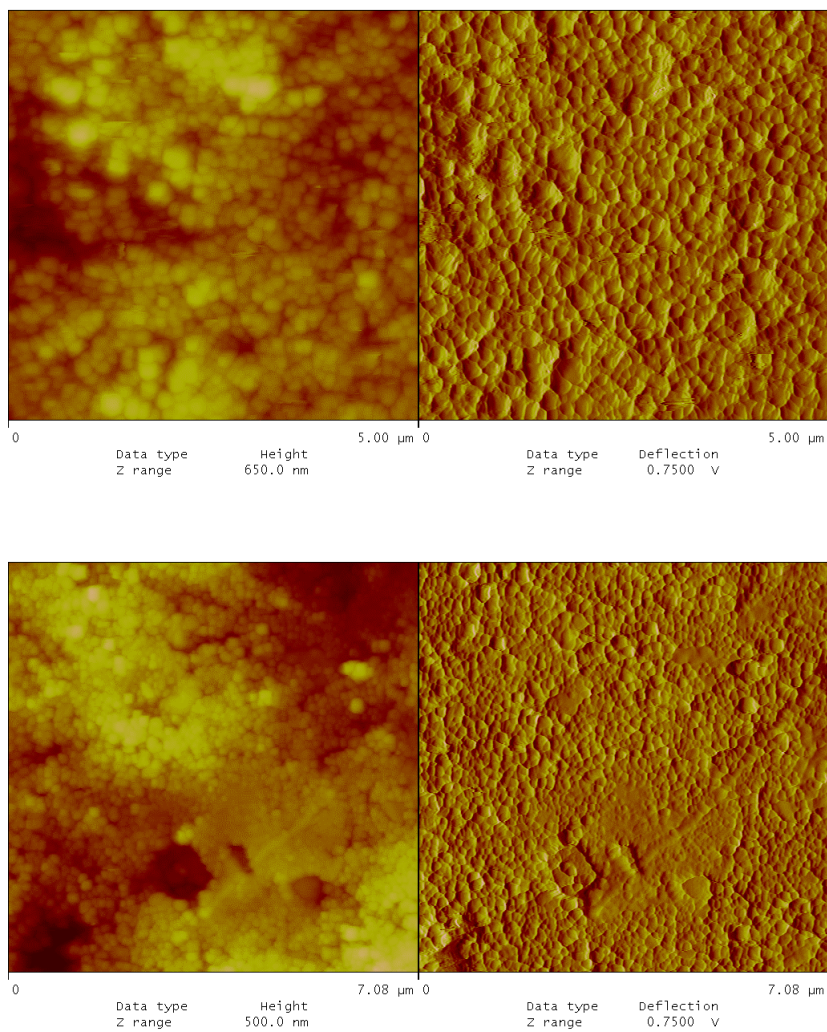


Figure 6. Top Figures: AFM in air in high mode (left) and force mode (right) of cathode surface in air, at different scan sizes. Samples were obtained from PDDA coated LMO powder. Bottom Figures: (in solution containing 30 mM PDDA). AFM in air in high mode (left) and force mode (right) of cathode surface in air, at different scan sizes. Samples were obtained from PDDA coated LMO powder (in solution containing 100 mM PDDA).

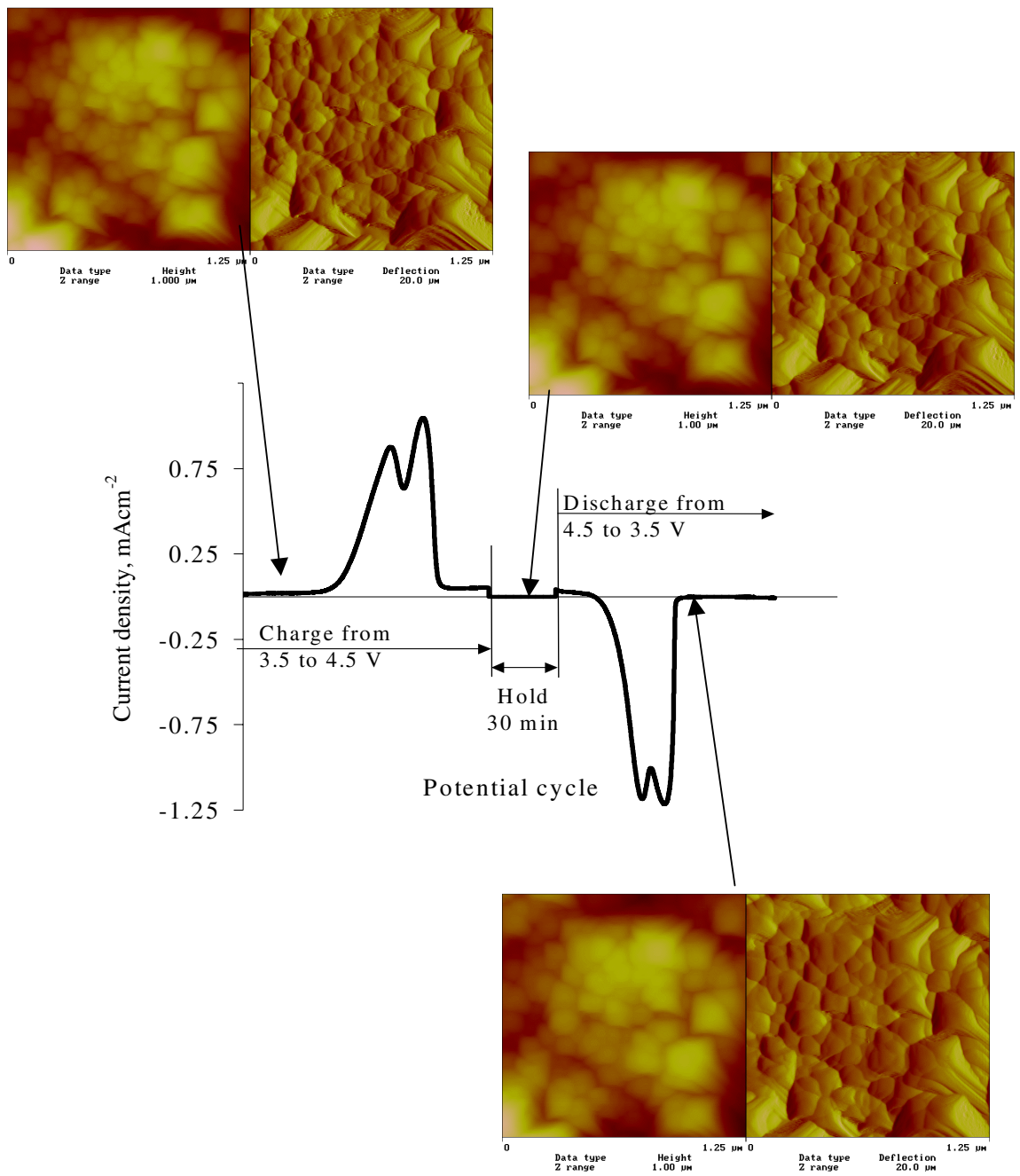


Figure 7. *In situ* EC-AFM of SM-LMO based cathode (30 mM PDDA solution) in 1 M LiPF₆ + EC/DEC electrolyte during charging from E = 3.5 V to E = 4.5 V, holding at 4.5 V for 1/2 h and discharging back to E = 3.5 V, at room temperature.

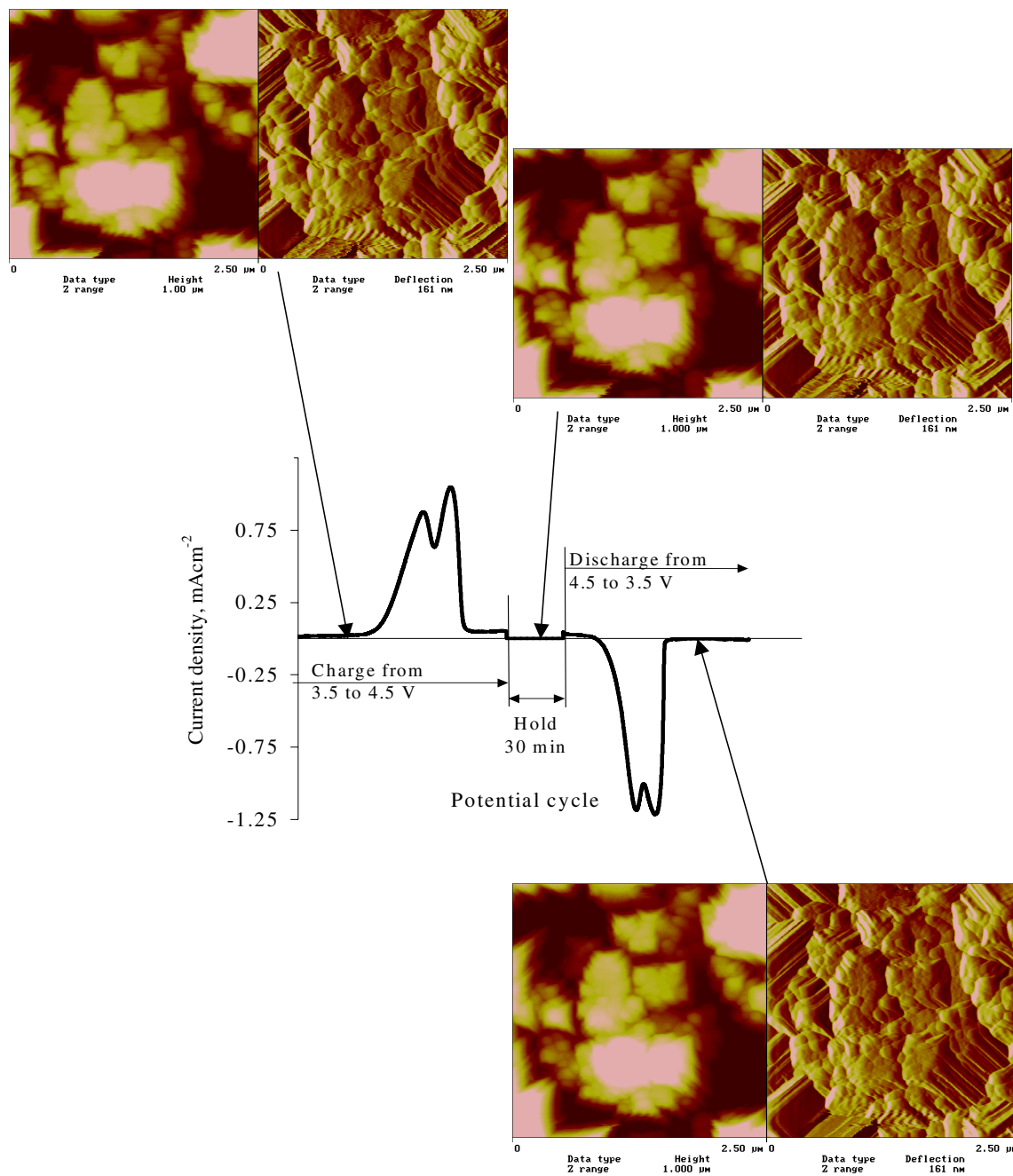


Figure 8. *In situ* EC-AFM of SM-LMO based cathode (30 mM PDDA solution) in 1 M LiPF₆ + EC/DEC electrolyte during charging from $E = 3.5$ V to $E = 4.5$ V, holding at 4.5 V for 1/2 h and discharging back to $E = 3.5$ V, at elevated temperature (55 °C).

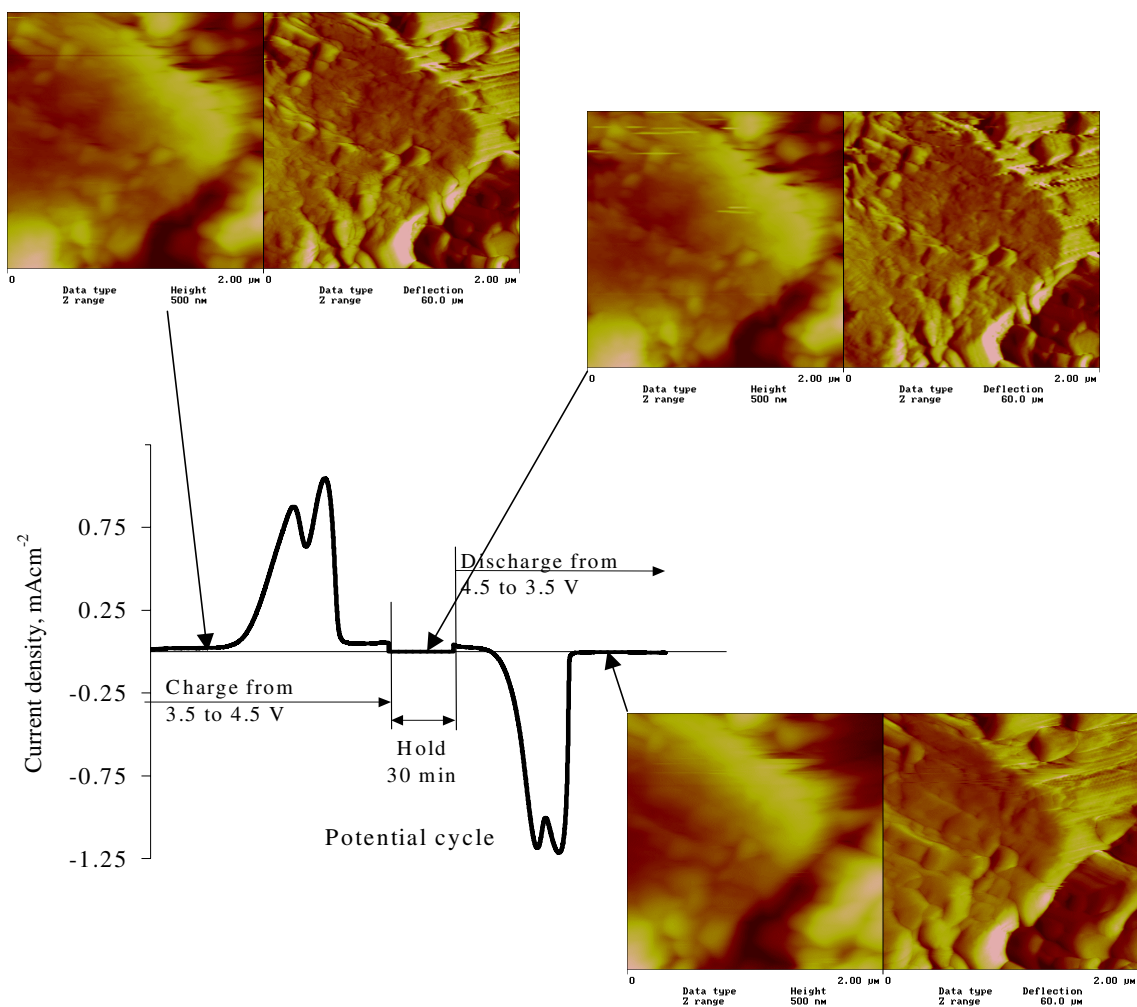


Figure 9 *In situ* EC-AFM of SM-LMO based cathode (100 mM PDDA solution) in 1 M LiPF_6 + EC/DEC electrolyte during charging from $E = 3.5$ V to $E = 4.5$ V, holding at 4.5 V for 1/2 h and discharging back to $E = 3.5$ V, at room temperature.

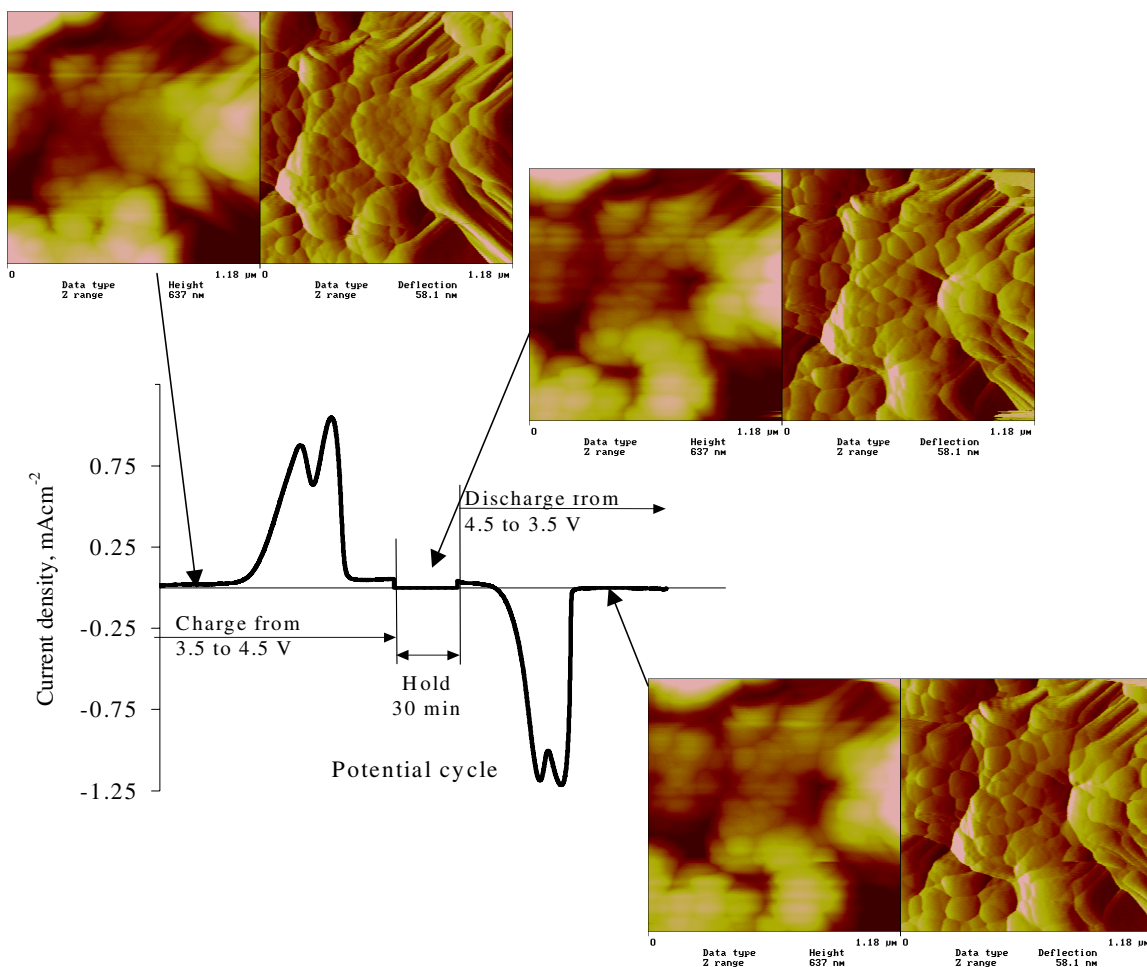


Figure 10

In situ EC-AFM of SM-LMO based cathode (100 mM PDDA solution) in 1 M LiPF_6 + EC/DEC electrolyte during charging from $E = 3.5$ V to $E = 4.5$ V, holding at 4.5 V for 1/2 h and discharging back to $E = 3.5$ V, at elevated temperature (55°C).

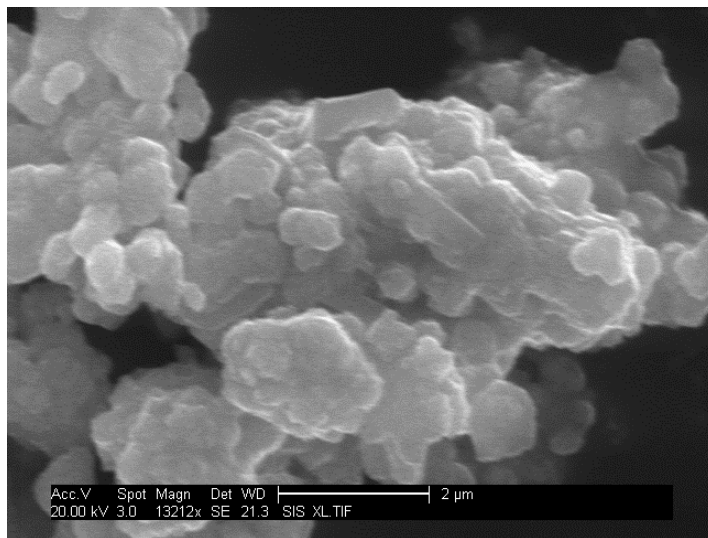


Figure 11. SEM image of LMO powder (before coating).

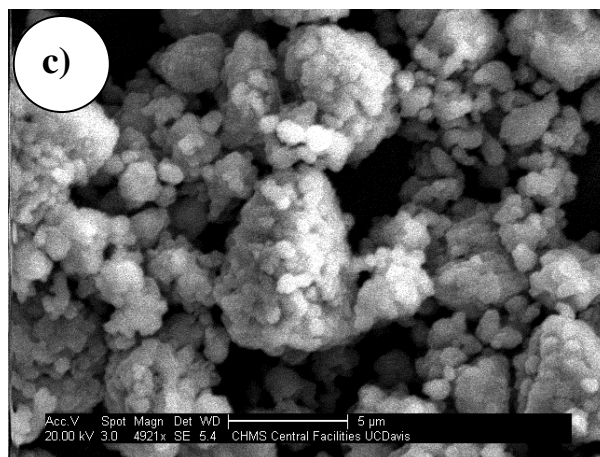
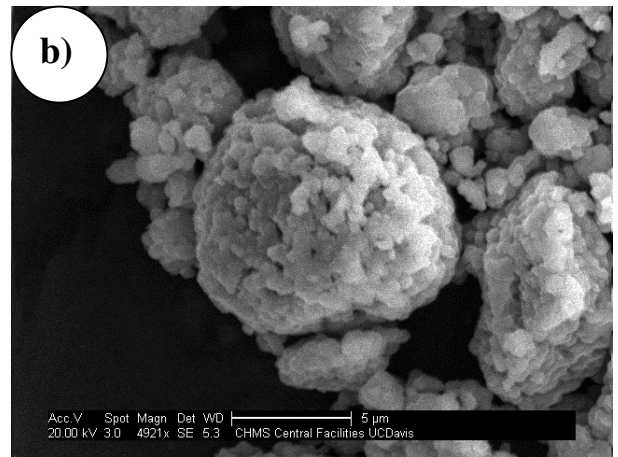
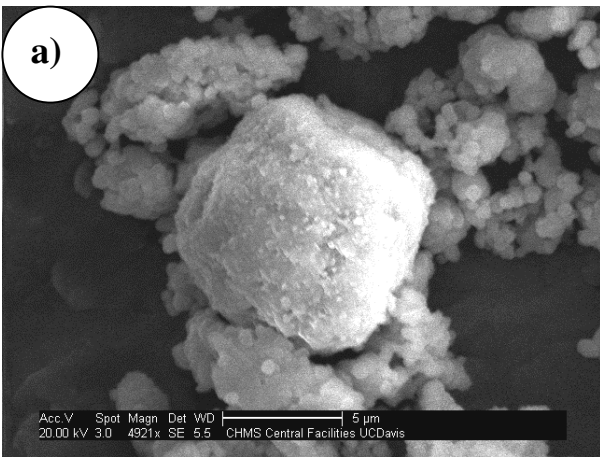


Figure 12. SEM images of PDDA coated powder in 10 (a), 30 (b) and 100 (c) mM PDDA solution.

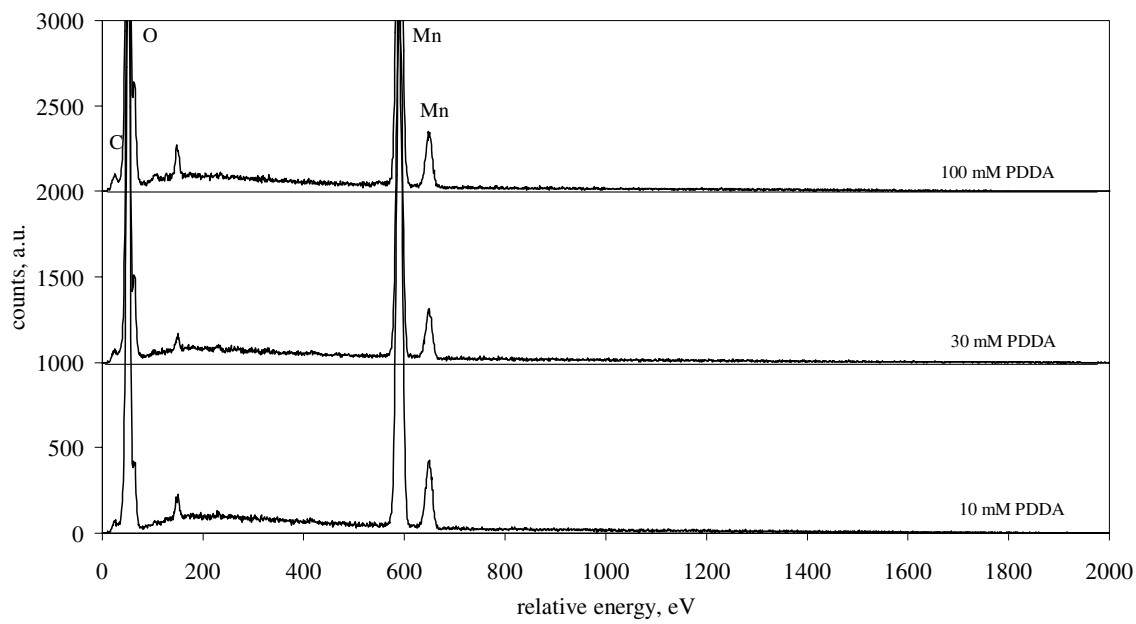


Figure 13 Comparison of EDAX data for PDDA coated powder in 10, 30 and 100 mM PDDA solution.

REFERENCES

1. Cho, J., Y. J. Kim, et al. (2000). "Novel LiCoO₂ cathode material with Al₂O₃ coating for a Li ion cell." *Chemistry of Materials* 12(12): 3788-3791.
2. Chowdari, B. V. R., G. V. S. Rao, et al. (2002). "Cathodic performance of anatase (TiO₂)-coated Li (Ni_{0.8}Co_{0.2})O₂." *Journal of Solid State Electrochemistry* 6(8): 565-567.
3. Kim, Y. J., T. J. Kim, et al. (2002). "The effect of Al₂O₃ coating on the cycle life performance in thin-film LiCoO₂ cathodes." *Journal of the Electrochemical Society* 149(10): A1337-A1341.
4. Sun, Y. K., K. J. Hong, et al. (2002). "Electrochemical performance of nano-sized ZnO-coated LiNi_{0.5}Mn_{1.5}O₄ spinel as 5 V materials at elevated temperatures." *Electrochemistry Communications* 4(4): 344-348.
5. Wang, Z. X., L. J. Liu, et al. (2002). "Structural and electrochemical characterizations of surface-modified LiCoO₂ cathode materials for Li-ion batteries." *Solid State Ionics* 148(3-4): 335-342.
6. Cho, J., Y. W. Kim, et al. (2003). "A breakthrough in the safety of lithium secondary batteries by coating the cathode material with AlPO₄ nanoparticles." *Angewandte Chemie-International Edition* 42(14): 1618-1621.
7. Kim, Y. J., H. Kim, et al. (2003). "Electrochemical stability of thin-film LiCoO₂ cathodes by aluminum-oxide coating." *Chemistry of Materials* 15(7): 1505-1511.
8. Wang, Z. X., X. J. Huang, et al. (2003). "Performance improvement of surface-modified LiCoO₂ cathode materials - An infrared absorption and X-ray photoelectron spectroscopic investigation." *Journal of the Electrochemical Society* 150(2): A199-A208.
9. Pistoia, G. and R. Rosati (1996). "Synthesis of an efficient LiMn₂O₄ for lithium-ion cells." *Journal of Power Sources* 58(2): 135-138.
10. Xia, Y. Y. and M. Yoshio (1996). "An investigation of lithium ion insertion into spinel structure Li-Mn-O compounds." *Journal of the Electrochemical Society* 143(3): 825-833.
11. Cho, J. P., J. Guan, et al. (1997). "Electrochemical properties of Li_xMn₂O₄ composite electrode in cells based on glass-polymer composite electrolytes." *Solid State Ionics* 95(3-4): 289-294.
12. Kang, S. H. and J. B. Goodenough (2000). "Li[Li_yMn_{2-y}]O₄ spinel cathode material prepared by a solution method." *Electrochemical and Solid State Letters* 3(12): 536-539.
13. Komaba, S., N. Kumagai, et al. (2001). "Manganese dissolution from lithium doped Li-Mn-O spinel cathode materials into electrolyte solution." *Electrochemistry* 69(10): 784-787.
14. Ma, Z. F., X. Q. Yang, et al. (2001). "Charge-discharge characteristics and phase transitions of mixed LiNi_{0.8}Co_{0.2}O₂ and LiMn₂O₄ cathode materials for lithium-ion batteries." *Journal of New Materials for Electrochemical Systems* 4(2): 121-125.
15. Quinlan, F. T., K. Sano, et al. (2001). "Surface characterization of the spinel Li_xMn₂O₄ cathode before and after storage at elevated temperatures." *Chemistry of Materials* 13(11): 4207-4212.
16. Xia, Y. Y., T. Sakai, et al. (2001). "Correlating capacity fading and structural changes in Li_{1+y}Mn_{2-y}O_{4-δ} spinel cathode materials - A systematic study on the effects of Li/Mn ratio and oxygen deficiency." *Journal of the Electrochemical Society* 148(7): A723-A729.

17. Yamane, H., T. Inoue, et al. (2001). "A causal study of the capacity fading of Li_{1.01}Mn_{1.99}O₄ cathode at 80 degrees C, and the suppressing substances of its fading." *Journal of Power Sources* 99(1-2): 60-65.
18. Aurbach, D., B. Markovsky, et al. (2002). "An analysis of rechargeable lithium-ion batteries after prolonged cycling." *Electrochimica Acta* 47(12): 1899-1911.
19. Lu, C. H. and S. W. Lin (2002). "Dissolution kinetics of spinel lithium manganate and its relation to capacity fading in lithium ion batteries." *Journal of Materials Research* 17(6): 1476-1481.
20. Shim, J., R. Kostecki, et al. (2002). "Electrochemical analysis for cycle performance and capacity fading of a lithium-ion battery cycled at elevated temperature." *Journal of Power Sources* 112(1): 222-230.
21. Wang, X. Q., H. Nakamura, et al. (2002). "Capacity fading mechanism for oxygen defect spinel as a 4 V cathode material in Li-ion batteries." *Journal of Power Sources* 110(1): 19-26.
22. Zhang, S. S. and T. R. Jow (2002). "Study of poly (acrylonitrile-methyl methacrylate) as binder for graphite anode and LiMn₂O₄ cathode of Li-ion batteries." *Journal of Power Sources* 109(2): 422-426.
23. Zheng, Z. S., Z. L. Tang, et al. (2003). "Review of cathode material LiMn₂O₄ for lithium ion batteries." *Journal of Inorganic Materials* 18(2): 257-263.
24. Wang, Z. X., C. A. Wu, et al. (2002). "Electrochemical evaluation and structural characterization of commercial LiCoO₂ surfaces modified with MgO for lithium-ion batteries." *Journal of the Electrochemical Society* 149(4): A466-A471.
25. Cho, J. (2001), "Stabilization of spinel-like phase transformation of o-LiMnO₂ during 55 degrees C cycling by sol-gel coating of CoO" *Chem Mater*, 13 (12): 4537-4541.
26. Amatucci GG, Blyr A, Sigala C, et al. (1997), "Surface treatments of Li_{1+x}Mn_{2-x}O₄ spinels for improved elevated temperature performance" *Solid State Ionics* 104 (1-2): 13-25.
27. Park SC, Kim YM, Kang YM, et al.(2001) "Improvement of the rate capability of LiMn₂O₄ by surface coating with LiCoO₂" *J Power Sources* 103 (1): 86-92.
28. Vidu R, Quinlan FT, Stroeve P. (2002), "Use of in situ electrochemical atomic force microscopy (EC-AFM) to monitor cathode surface reaction in organic electrolyte" *Ind Eng Chem Res* 41 (25): 6546-6554
29. P. Brandani and P. Stroeve. Adsorption and Desorption of PEO-PPO-PEO Triblock Copolymers on a Self-Assembled Hydrophobic Surface. *Macromolecules*, 36: 9492-9501, 2003.

LIST OF FIGURES

- Figure 1. Charge/discharge curves and of LMO-based cathode in 1 mol of LiPF₆ + EC/DEC.
- Figure 2. Charge/discharge curves (a) and the variation of the measured capacity with the number of cycles (b) for the cathode obtained from PDDA coated powder in 50 mM PDDA solution
- Figure 3. Variation of the measured capacity during charging (a) and discharging (b) with the number of cycles for the cathodes obtained from the PDDA coated powder.

- Figure 4. Charge/discharge curves of SM-LMO (30 mM PDDA) -based cathode before (a) and after (b) storage.
- Figure 5. TEM image (x49K) of typical SM-LMO powder indicating crystalline LiMn_2O_4 region and polymeric film.
- Figure 6. Top Figures: AFM in air in high mode (left) and force mode (right) of cathode surface in air, at different scan sizes. Samples were obtained from PDDA coated LMO powder. Bottom Figures: (in solution containing 30 mM PDDA). AFM in air in high mode (left) and force mode (right) of cathode surface in air, at different scan sizes. Samples were obtained from PDDA coated LMO powder (in solution containing 100 mM PDDA).
- Figure 7. In situ EC-AFM of SM-LMO based cathode (30 mM PDDA solution) in 1 M LiPF_6 + EC/DEC electrolyte during charging from $E = 3.5$ V to $E = 4.5$ V, holding at 4.5 V for 1/2 h and discharging back to $E = 3.5$ V, at room temperature.
- Figure 8. In situ EC-AFM of SM-LMO based cathode (30 mM PDDA solution) in 1 M LiPF_6 + EC/DEC electrolyte during charging from $E = 3.5$ V to $E = 4.5$ V, holding at 4.5 V for 1/2 h and discharging back to $E = 3.5$ V, at elevated temperature (55°C).
- Figure 9. In situ EC-AFM of SM-LMO based cathode (100 mM PDDA solution) in 1 M LiPF_6 + EC/DEC electrolyte during charging from $E = 3.5$ V to $E = 4.5$ V, holding at 4.5 V for 1/2 h and discharging back to $E = 3.5$ V, at room temperature.
- Figure 10. In situ EC-AFM of SM-LMO based cathode (100 mM PDDA solution) in 1 M LiPF_6 + EC/DEC electrolyte during charging from $E = 3.5$ V to $E = 4.5$ V, holding at 4.5 V for 1/2 h and discharging back to $E = 3.5$ V, at elevated temperature (55°C).
- Figure 11. SEM image of LMO powder (before coating).
- Figure 12. SEM images of PDDA coated powder in 10 (a), 30 (b) and 100 (c) mM PDDA solution.
- Figure 13. Comparison of EDAX data for PDDA coated powder in 10, 30 and 100 mM PDDA solution.